Adaptive Hysteresis Compensation for a Magneto-Rheological Robot Actuator*

Peyman Yadmellat and Mehrdad R. Kermani

Abstract— In this paper, adaptive compensation of the hysteresis in a Magneto-Rheological (MR) fluid based actuators and its application for sensor-less high fidelity force/torque control is investigated. The MR actuator considered in this paper was originally described in [1] and [2]. This actuator offers high torque-to-mass and torque-to-inertia ratios. Yet, as an essential component of MR actuators, the magnetic circuit of the actuator shows hysteresis between its input current/voltage and output magnetic field. The hysteresis in the magnetic circuit results in a similar relationship between the input current and the output torque of the MR actuator. The control scheme used with actuators possessing hysteresis often requires compensating for the hysteresis. To this end, we propose an adaptive control method based on feedback linearization that estimates both hysteresis and uncertain parameters of the magnetic circuit. A set of experiments is performed to validate the effectiveness of the proposed method.

I. INTRODUCTION

Magneto-Rheological (MR) fluids are a special class of fluids that exhibit variable yield stress with respect to an applied magnetic field. MR fluids offer unique properties enabling their use in variety of electro-mechanical devices. The states of MR fluids can vary from a fluid to a semi-solid (or plastic) state upon exposing to a magnetic field, with the ability to achieve up to 100 kPa yield stress in a matter of few milliseconds. Their controllability and fast responses to external magnetic field have made MR fluids an attractive technology for a broad range of applications from civil engineering to automotive, robots, and rehabilitation applications (e.g. see [3]–[5]).

Benefits of a controllable actuator utilizing MR fluids has been recognized in multiple robot applications. Design and development of several haptic devices based on MR fluids were presented in [6]–[8]. It has been shown that the actuation performance can be enhanced using MR actuators both in robot manipulators [9] and haptic devices [10]. The advantages of MR actuators in variable impedance actuation were discussed in [11], [12]. Moreover, it has been verified that MR actuators are beneficial in improving safety of human-friendly robots due to their intrinsic passivity [1], [13].

The main difficulty in employing MR actuators in robotic applications lies in the nonlinear behavior of the actuator due to the use of ferromagnetic materials in the magnetic circuit

of the fluid. The magnetic circuit introduces hysteresis in the current–torque curve of the actuator. The Greek word "Hysteresis" means "to lag behind", and it describes a relationship between the inputs and outputs of a certain system. For a single-input, single-output system, hysteresis is the presence of a non-degenerate input-output closed curve as the frequency of excitation tends toward dc [14]. The presence of hysteresis leads to such known problems in control systems as tracking errors, unwanted harmonics, and instability [15]. A high gain feedback control can compensate for the negative effects of the hysteresis [16]. However, high gain feedbacks often result in more power consumption and poor control performance. To compensate for the hysteresis, a hysteresis model is often required in designing the control algorithm. The accuracy of the model plays an important role in the effectiveness of the control and enhancing the system performance.

In hysteresis modeling two main approaches, namely a) phenomenological modeling and b) physic-based modeling are often discussed. Phenomenological models include Preisach [17], [18], Prandtl-Ishlinskii [19], and Krasnoselskii-Pokrovskii [20] models. Although these models are widely accepted and can successfully predict magnetic hysteresis, they present several implementation problems that restrict their applications for the systematic design of closed-loop controllers [21]. Moreover, the formulation of phenomenological models is based on prior experimental measurements, that makes the use of such models controversial in applications in which reliability and/or robust performance of the control are of primary importance. Alternative methods are analytical models built on physical principles of the magnetic systems. Jiles-Atherton's model [22] and Hodgdon's model [23] are examples of such models for ferromagnetic hysteresis. Jiles-Atherton's model was applied in [24] to analysis the magnetic hysteresis of an MR actuator. Hodgdon's hysteresis model was also used to predict the magnetic circuit behaviors of an MR actuator in [9].

While these models have been used for either off-line simulations or actuator designs, to the best of our knowledge, no real-time implementation of the above mentioned models has ever been reported for the control design purposes. The mentioned models have either been used for off-line simulations or the design of the actuators but not in the design of a real-time controller. Given the fact that most non-model based controllers proposed in the literature (e.g. PID[1] controller in [25]) result in poor performance, the need for a

The Authors are with the Electrical and Computer Engineering Department, the University of Western Ontario, London, ON N6A 5B9 Canada `pyadmell@uwo.ca`, `mkermani@eng.uwo.ca`.

[1]Proportional-Integral-Derivative

model-based controller for utilizing MR actuators is apparent for achieving high performance and delivering high-fidelity force/torque control.

The main contribution of this paper is the design of a new closed-loop control for actuators with hysteretic behavior. A new adaptive controller is proposed to deal with *uncertainties* of MR actuators. In the design of the controller, both geometrical parameters of the actuators and physics of the system are considered in order to compensate for the hysteretic and nonlinear behaviors of MR actuators. The main advantage of the proposed controller is that it requires only the estimation of the output torque eliminating the need for additional force/torque sensors in the control loop. This sensor-less force/torque control technique offers significant advantages in terms of cost reduction and performance improvement thanks to unique properties of MR fluids. The stability of the closed-loop system is rigorously analyzed and the conditions on which the system remains stable are derived. The proposed scheme is experimentally validated using two test benches including a 1-DOF robot arm and a 2-DOF planar robot with antagonistic MR actuation. Furthermore, our sensor-less force/torquee control results are compared to those obtained using direct force/torque measurements and the advantages are highlighted.

The rest of this paper is organized as follow: Section II introduces MR fluids along with their applications in electro-mechanical actuators. Section III discusses the characteristics of MR fluids, and their controllable yield stress. Dynamic models of the magnetic circuit and the torque-current relationship in MR actuators are also described in this section. Section IV presents our proposed adaptive control method. In Section V, experimental results for torque control are presented. Finally, Section VI concludes the paper.

II. MAGNETO-RHEOLOGICAL ACTUATORS

The Magneto-Rheological (MR) effect was discovered by Jacob Rabinow in 1940s who developed the first MR-based device [26] at the US National Bureau of Standards. MR fluids are non-homogenous suspensions of micrometer-sized ferromagnetic particles in a carrier fluid. The apparent viscosity of MR fluids can be adjusted by magnetic fields. The suspended particles in these fluids form columns (chains) aligned to the direction of the applied field that results in shearing or flow resistance in the fluid. The degree of the resistive force is related to the strength of the magnetic field, resulting in a field dependent yield stress in MR fluids [27], [28]. In the absence of a magnetic field, MR fluids act as Newtonian fluids, whose viscosity changes proportionally to the shear rate.

The operational modes of MR-based devices can mainly be categorized into three different modes; flow mode (also know as valve mode), direct shear mode, and squeeze film mode [29]–[31], as demonstrated in Fig. 1. Linear and rotary MR actuators (e.g. clutches, brakes, and dampers) utilize either the flow mode [32], shear mode [33], or a combination of both [34], [35], while squeeze mode can be used for axial or rotary operations with limited torque/force capacity
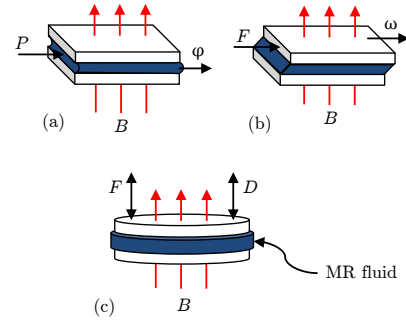

Fig. 1.　Operation modes of MR fluids; (a)flow mode, (b) direct shear mode, and (c)squeeze film mode, where F, P, φ, D, ω, and B represents force, pressure, flow, displacement, velocity, and the applied magnetic field, respectively.
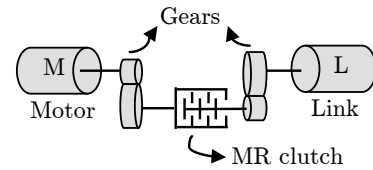

Fig. 2.　A possible arrangement for robot joint actuation using an MR clutch.

[36]. The characteristics of MR actuators depend on the mode in which the actuator operates, and differ from one type to another. Our focus in this paper is only on MR clutches and their application for force/torque control in robotics. MR clutches can be employed in the actuation mechanism of robot manipulators to control the delivery of output torque at the joints. Fig. 2 depicts a possible arrangement for actuating a robot joint. The active drive (i.e. motor) provides power to the joint via an MR clutch that controls the output torque. The advantages of using MR clutches in robot control were studied in [37]. The utilization of MR clutches at robot joints enhances the robot performance while reducing the impedance for more human-friendly actuation. The high torque-to-mass ratio and fast transient response in both position and torque control modes are among other benefits of MR fluid based actuation.

III. MR ACTUATOR MODEL

Fig. 3 shows the cross–section of a typical multi–disk MR clutch. The input shaft breaks out into a set of input disks which are aligned in parallel to a set of output disks attached to the output shaft. MR fluid fills the volume between input and output disks. By energizing the electromagnetic coil, the apparent viscosity of MR fluids, thereby the compliance of the clutch can be controlled. A model for an MR clutch based actuation should consist of two parts; a) the MR clutch magnetic circuit that relates the input current to the resultant magnetic field, and b) the mechanical dynamics of the MR clutch that relates the output torque of the actuator to its internal magnetic field. In what follows we describe each of these parts in more details.
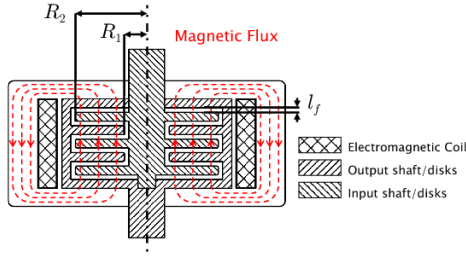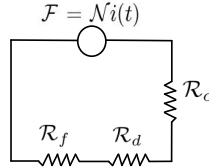
Fig. 3.   Cross-section of a multi-disk MR clutch.

Fig. 4.   Magnetic circuit of an MR clutch.

A. MR Clutch Magnetic Circuit Model

Fig. 4 shows a simplified model of the magnetic circuit of a typical MR clutch, where $\mathcal{R}_c$, $\mathcal{R}_f$, and $\mathcal{R}_d$ are the reluctance of the core, the gaps between the disks, and the disks, respectively. Assuming the magnetic field is uniform, steady, and perpendicular to the cross sectional area of A, the magnetic field intensity H can be calculated as below,

$$H = \frac{\Phi}{\mu A}, \tag{1}$$

where Φ is the magnetic flux in the circuit obtained based on the total reluctance of the circuit $\mathcal{R}_t$, the number of winding $\mathcal{N}$, and the input current $i(t)$.

The flux variation $\dot{\Phi}$ caused by an alternating input current results in an induced magnetic field H_d in opposite direction of the applied magnetic field based on the Farady-Lenz law. The flux variation is equivalent to the magnetic field density variation $\dot{B}$ that is related to the induced magnetic field as $H_d = -\lambda \dot{B}$, where λ depends on the geometry of the magnetic circuit. Hence, the effective magnetic field H_{eff} equals to the sum of the applied field H and the induced field H_d, i.e.,

$$H_{\text{eff}} = H - \lambda \dot{B}. \tag{2}$$

In ferromagnetic materials, the B-H curve can be explained by a nonlinear and hysteretic relation as $B \in \mathcal{B}(H_{\text{eff}})$, where $\mathcal{B}$ is a suitable hysteresis operator [19, ch. 2]. Considering (2), the magnetic circuit behavior of an MR clutch indicates a rate-dependent hysteresis.

B. MR Clutch Mechanical Model

It is recognized that the typical relationship between shear stress and shear rate in Bingham fluids can imitate the behavior of MR fluids under an applied magnetic field [28], [38], [39]. In this regard, Shames and Cozzarelli [40] developed an idealized mechanical model known as Bingham

visco–plastic model. This model describes the rheological properties of MR fluids. Based on this model, a visco–plastic model for a typical multi-disk clutch can be obtained as a function of the yield stress in MR fluids and the relative velocity between the input and output shafts [1].

According to this model, the shear stress of the fluid is given by,

$$\tau = \tau_y(B) + \eta \dot{\gamma}(r), \quad \tau > \tau_y, \tag{3}$$

where τ is the shear stress, τ_y is the field dependent yield stress, B is the magnetic field density, η is the Newtonian viscosity, the shear rate $\dot{\gamma} = \omega r l_f^{-1}$, ω is the angular velocity between the input and output shafts of the clutch, and l_f is the gap between the input and output disks. Data relating the yield stress of MR fluids to applied magnetic fields is generally provided by the manufacturers (e.g. LORD Co.).

It is easy to show that the torque produced by a circumferential element at a radius r is given by,

$$dT = 2\pi r^2 \tau dr. \tag{4}$$

Assuming that the clutch has N output disks, the torque transmitted through the clutch can be obtained after substituting (3) into (4) and integrating across both faces of each output disk, i.e.,

$$
\begin{aligned}
T &= 2N \int_{R_1}^{R_2} 2\pi \left(\tau_y(B) r^2 + \eta \frac{\omega r^3}{l_f} \right) dr \\
&= 4N\pi \left(\frac{\tau_y(B) \left(R_2^3 - R_1^3 \right)}{3} + \frac{\eta \omega \left(R_2^4 - R_1^4 \right)}{4 l_f} \right),
\end{aligned}
\tag{5}
$$

where R_1 and R_2 are the inner and outer radii of the disks, respectively. All other parameters are as defined previously. The viscosity η of the carrier fluid is typically in the range of 0.1 to 0.3 Pa-s.

IV. TORQUE CONTROL FOR MR CLUTCH BASED ACTUATION

In this section force/torque control using an MR actuator is discussed. Using (2) and (5), the torque-current relationship can be written as follows,

$$
\begin{aligned}
\dot{B} &= -\lambda^{-1} \mathcal{H}(B) + \vartheta i(t), \\
T &= \wp_1 \tau_y(B) + \wp_2 \omega,
\end{aligned}
\tag{6}
$$

where $\mathcal{H} = \mathcal{B}^{-1}$ is a hysteresis operator to be determined, $\vartheta = \lambda^{-1} \mathcal{N} / (\mu A \mathcal{R}_t)$, and $\wp_1$ and $\wp_2$ are the geometrical parameters defined as defined in Section III-B.

Let $e_T(t) = T_d(t) - T(t)$ be the control error, where T_d is the desired torque. Then, the control error dynamic is given by,

$$
\begin{aligned}
\dot{e}_T(t) &= \dot{T}_d(t) - \wp_2 \dot{\omega} \\
&\quad + \left(\wp_1 \lambda^{-1} \mathcal{H}(B) - \wp_1 \vartheta i(t) \right) \left(\partial \tau_y(B) / \partial B \right).
\end{aligned}
\tag{7}
$$

Assuming all parameters of the system are known, $i(t)$ can be chosen so as to linearize the system described in (7), i.e.,

$$
\begin{aligned}
i(t) &= \left(\wp_1 \vartheta \left(\partial \tau_y(B) / \partial B \right) \right)^{-1} \left(\wp_1 \lambda^{-1} \mathcal{H}(B) (\partial \tau_y(B) / \partial B) \right. \\
&\quad \left. + \dot{T}_d(t) - \wp_2 \dot{\omega} + a e_T \right),
\end{aligned}
\tag{8}
$$

where $a > 0$ is a constant scalar. However, $\mathcal{H}(B)$, λ^{-1}, and ϑ are unknown, and the input control law given in (8) cannot be constructed in practice.

Let us assume that the nonlinear function $\lambda^{-1}\mathcal{H}(B)$ can be represented as,

$$\lambda^{-1}\mathcal{H}(B) = \mathcal{H}_\lambda(B) + \epsilon(B), \qquad (9)$$

where $\epsilon(B)$ is a bounded approximation error, i.e. $||\epsilon(B)|| \leq \bar{\epsilon}$, and $\mathcal{H}_\lambda(B)$ is a polynomial of degree m, i.e.,

$$\mathcal{H}_\lambda(B) = \sum_{i=0}^{m} \alpha_i B^i, \qquad (10)$$

in that α_i, $(i = 1, 2, ..., m)$ represents the unknown parameters to be estimated. As such, $\mathcal{H}_\lambda(B)$ can be approximated as,

$$\hat{\mathcal{H}}_\lambda(B) = \sum_{i=0}^{m} \hat{\alpha}_i B^i, \qquad (11)$$

To cope with the uncertainties in (8), the $\lambda^{-1}\mathcal{H}(B)$ and ϑ^{-1} can be replaced by their estimates as

$$
\begin{aligned}
\hat{i}(t) &= \left(\wp_1 \hat{\vartheta} \left(\partial \tau_y(B)/\partial B \right) \right)^{-1} (\dot{T}_d(t) - \wp_2 \dot{\omega} \\
&\quad + a e_T + \wp_1 \hat{\mathcal{H}}_\lambda(B)(\partial \tau_y(B) \partial B)).
\end{aligned}
\qquad (12)
$$

Introducing the control law given in (12) into (7) leads to the following control error dynamics,

$$
\begin{aligned}
\dot{e}_T(t) &= \dot{T}_d(t)(1 - \vartheta \hat{\vartheta}^{-1}) - \wp_2 \dot{\omega}(1 - \vartheta \hat{\vartheta}^{-1}) \\
&\quad + \wp_1(\partial \tau_y(B) \partial B) \left(\mathcal{H}_\lambda(B) - \hat{\mathcal{H}}_\lambda(B) \vartheta \hat{\vartheta}^{-1} \right) \\
&\quad - \vartheta \hat{\vartheta}^{-1} e_T + \wp_1 \epsilon(B)(\partial \tau_y(B) \partial B).
\end{aligned}
\qquad (13)
$$

By adding and subtracting $a e_T + \wp_1(\partial \tau_y(B)/\partial B)\hat{\mathcal{H}}_\lambda(B)$ to and from (13) and after some algebraic manipulations the new control error dynamics can be written as follows using (10) and (11),

$$
\begin{aligned}
\dot{e}_T(t) &= -a e_T + u_c(1 - \vartheta \hat{v}) \\
&\quad + \wp_1(\partial \tau_y(B)/\partial B) \left(\sum_{i=0}^{m} \tilde{\alpha}_i B^i + \epsilon(B) \right)
\end{aligned}
\qquad (14)
$$

where $\hat{v} = \hat{\vartheta}^{-1}$ and $u_c = \dot{T}_d - \wp_2 \dot{\omega} + \wp_1 \hat{\mathcal{H}}_\lambda(B)(\partial \tau_y(B) \partial B) + a e_T$ and $\tilde{\alpha}_i = \alpha_i - \hat{\alpha}_i$, $(i = 0, 1, ..., m)$.

The main result of this section is given in the following theorem.

Theorem 1: Assuming the sign of ϑ, i.e. $sgn(\vartheta)$, is known[2], if the control input (12) is applied to the system described in (6), and the polynomial coefficients $\hat{\alpha}_i$, $(i = 0, 1, ..., m)$ and the parameter $\hat{v}$ are updated according to the following rules,

$$\dot{\hat{v}} = sgn(\vartheta) \iota u_c e_T, \qquad (15)$$

$$\dot{\hat{\alpha}}_i = \wp_1 \left(\partial \tau_y(B)/\partial B \right) \kappa e_T B^i, \qquad (16)$$

[2]The sign of ϑ can be easily found by applying a step input current to the coil (see (6)).

where $\iota > 0$ and $\kappa > 0$ are the adaption gains, then the control error e_T is uniformly ultimately bounded, i.e. $|e_T| \leq \rho$, in that ρ is inversely proportional to the control parameter a in (12), and can be made arbitrarily small.

Proof: Consider the following Lyapunov function candidate,

$$V = \frac{1}{2}\{ e_T^2 + |\vartheta| \iota^{-1} \tilde{v}^2 + \kappa^{-1} \sum_{i=0}^{m} \tilde{\alpha}_i^2 \}, \qquad (17)$$

where

$$\tilde{v} = v - \hat{v} = \vartheta^{-1} - \hat{\vartheta}^{-1},$$

the time derivative of (17) is given by,

$$\dot{V} = e_T \dot{e}_T + |\vartheta| \iota^{-1} \tilde{v} \dot{\tilde{v}} + \kappa^{-1} \sum_{i=0}^{m} \tilde{\alpha}_i \dot{\tilde{\alpha}}_i, \qquad (18)$$

By substituting (14) and (15) into (18), one can obtain,

$$
\begin{aligned}
\dot{V} &= -a e_T^2 + \kappa^{-1} \sum_{i=0}^{m} \tilde{\alpha}_i \dot{\tilde{\alpha}}_i \\
&\quad + \wp_1 e_T \left(\partial \tau_y(B)/\partial B \right) \left(\sum_{i=0}^{m} \tilde{\alpha}_i B^i + \epsilon(B) \right)
\end{aligned}
\qquad (19)
$$

Furthermore, introducing (16) into (19), the following inequality holds,

$$
\begin{aligned}
\dot{V} &= -a e_T^2 + \wp_1 e_T \epsilon(B) \left(\partial \tau_y(B)/\partial B \right) \\
&\leq -a e_T^2 + \wp_1 \bar{\epsilon} \bar{\delta}_{\tau_y} |e_T|,
\end{aligned}
\qquad (20)
$$

where $|\partial \tau_y(B)/\partial B| \leq \bar{\delta}_{\tau_y}$. Hence, $\dot{V}$ is negative semi-definite outside the region χ with a bound ρ specified as $\chi = \{ e_T | \ |e_T| \geq \rho \}$, where $\rho = \wp_1 \bar{\epsilon} \bar{\delta}_{\tau_y}/a$. Obviously, if e_T occurs in a region where $\dot{V} > 0$, then e_T will increase such that it will eventually move outside the region χ, where $\dot{V}$ is negative semi-definite. This implies that V (or equivalently e_T) will reduce. Therefore, ρ can be considered as a bound on the control error e_T. This completes the proof of the theorem. ∎

V. EXPERIMENTAL VALIDATION

In this section, the performance of the proposed control method is examined by performing several experiments. The proposed method only uses magnetic field measurements, and control the output torque by adjusting the input current. No force feedback is used in the construction of the proposed controller, and torque measurements are only provided for the sake of comparison. To highlight the advantages of the proposed method, we also implemented a PID controller whereby the output torque is regulated by using force feedbacks. Two 1-DOF and 2-DOF manipulators were utilized as our experimental platforms. In both platforms, a static load cell (Transducer Techniques SBO-1K) was incorporated for torque measurements.
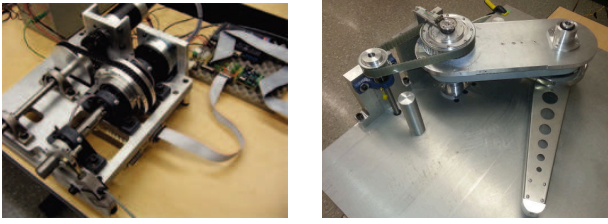
Fig. 5.   The 1-DOF and 2-DOF platforms.

Fig. 7.   Torque control results for 1 Hz sinusoid desired trajectory.

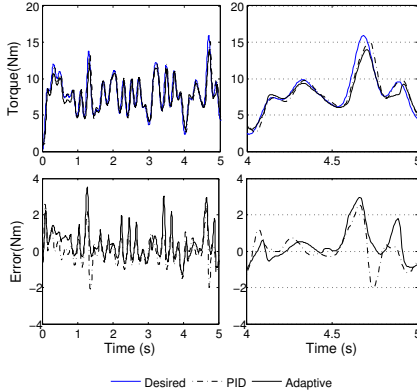Fig. 8.   Torque control results for 5 Hz sinusoid desired trajectory.

Fig. 6.   Torque control results for 1-DOF manipulator corresponding to Multi-Sinusoids desired torque trajectory. The left column shows the zoomed-in to a shorter time interval.

A. 1-DOF Manipulator

The 1-DOF manipulator (see Fig. 5) used in this section utilizes an MR clutch in its core. The MR clutch has the torque capacity of 75 Nm. The MR clutch is driven by a servo amplifier (Maxon 4-Q-DC Servo-amplifier ADS 50/5) set up in torque mode to provide the command current. A servo motor (Maxon EC 60) provides the rotational input to the MR clutch. In our experiment, the adaptive controller and a PID controller were implemented on a desktop computer to control the actuator via a National Instruments (NI USB-6229) multifunction I/O device. The sampling frequency for gathering experimental data is set to 250 Hz. Using this setup, a standard Multi-Sinusoids desired torque was considered. The desired trajectory was obtained using 10 different frequencies distributed uniformly between 0.75 Hz to 5 Hz. Fig. 6 compares the results for the adaptive controller and the PID controller. Parameters in the PID controller are also optimized to obtain the best result. As observed, the proposed adaptive method is capable of controlling the output torque very accurately after reasonably short transition (adaption) time. Also, the result shows that the proposed control scheme can be as accurate as a controller which uses force feedback.

B. 2-DOF Planar Manipulator

The 2-DOF manipulator utilises antagonistic actuation using two MR clutches at the first joint, and a combination of an MR clutch and a constant force spring at the second joint. The manipulator is driven by a brushless motor
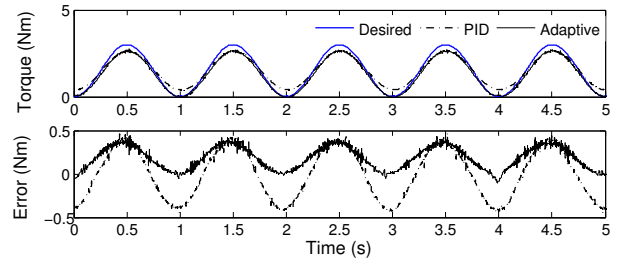
(BLWRPG235D-36V-4000-R13) for providing the rotational inputs to the MR clutches. The motor was driven by a driver in velocity control mode. The manipulator incorporates two encoders (HEDS-9000). Three high-power motor drivers, set in current mode, provide the command currents to the MR clutches (AMC-AZ12A8). In our experiment, the proposed controller is implemented on a desktop computer, controlled the manipulator via a dSPACE (DS 1103) controller board. The sampling frequency for gathering experimental data was set to 1 kHz.

In this set of experiments, the torque control of the first joint is considered. Figs. 7 and 8 show the adaptive control results, respectively, for 1 and 5 Hz desired sinusoids in comparison with that of the PID. Although, force feedback measurements were used for the PID controller, the adaptive controller performs more accurate tracking in both cases. Root Mean Square Errors (RMSEs) for the adaptive control is 0.2243 Nm (at 1 Hz) and 0.2365 Nm (at 5 Hz), while they are 0.2776 Nm (at 1 Hz) and 0.2914 Nm (at 5 Hz) for the PID controller. More accurate results are also expected by optimising the parameters in the adaption rules.

VI. CONCLUSION

A new closed-loop control was proposed in this paper for actuators with hysteretic behavior. A new adaptive controller was designed to deal with the *un-modeled* hysteresis and *uncertainties* in MR actuators with insight into physical principles of the actuators. The hysteresis was approximated using a polynomial function, where adaption rules were provided to estimate the unknown parameters. The controller was constructed based on magnetic field measurements only, and no force feedback measurements were used. The stability

of the closed-loop system was evaluated using Lyapunov method. The main benefit of the controller is that it can reduce the manufacturing cost by eliminating the need for additional force/torque sensors in the control loop. It is also expected to achieve higher performance by addressing fundamental problems with the stiff force sensors. The proposed scheme was also validated experimentally using two test benches. The sensor-less torque control results were also compared to those obtained using direct torque measurements. The results illustrated an accurate and competitive control performance. Further results on force control as well as hybrid force/position control will be provided as part of our ongoing research.

REFERENCES

[1] A. S. Shafer and M. R. Kermani, "On the feasibility and suitability of mr and er based actuators in human friendly manipulators," in *Intelligent Robots and Systems, 2009. IROS 2009. IEEE/RSJ International Conference on.* IEEE, 2009, pp. 2904–2909.

[2] P. Yadmellat, A. S. Shafer, and M. R. Kermani, "Development of a safe robot manipulator using a new actuation concept," in *Robotics and Automation (ICRA), 2013 IEEE International Conference on.* IEEE, 2013, pp. 337–342.

[3] O. Ashour, C. A. Rogers, and W. Kordonsky, "Magnetorheological fluids: Materials, characterization, and devices," *Journal of Intelligent Material Systems and Structures*, vol. 7, no. 2, pp. 123–130, March 1996.

[4] D. J. Peel, R. Stanway, and W. A. Bullough, "Experimental study of an er long-stroke vibration damper," in *Smart Structures and Materials 1997: Passive Damping and Isolation*, L. P. Davis, Ed., vol. 3045, no. 1. SPIE, 1997, pp. 96–107.

[5] J. D. Carlson and D. M. Catanzarite, "Magnetorheological fluid devices and process of controlling force in exercise equipment utilizing same," October 1998.

[6] A. Bicchi, M. Raugi, R. Rizzo, and N. Sgambelluri, "Analysis and design of an electromagnetic system for the characterization of magnetorheological fluids for haptic interfaces," *Magnetics, IEEE Transactions on*, vol. 41, no. 5, pp. 1876–1879, 2005.

[7] B. Liu, W. Li, P. Kosasih, and X. Zhang, "Development of an mr-brake-based haptic device," *Smart materials and structures*, vol. 15, no. 6, p. 1960, 2006.

[8] F. Ahmadkhanlou, G. N. Washington, Y. Wang, and S. E. Bechtel, "The development of variably compliant haptic systems using magnetorheological fluids," in *12th SPIE International Symposium, San Diego, CA*, 2005.

[9] J. An and D.-S. Kwon, "Modeling of a magnetorheological actuator including magnetic hysteresis," *Journal of Intelligent Material Systems and Structures*, vol. 14, no. 9, pp. 541–550, September 2003.

[10] *Haptic experimentation on a hybrid active/passive force feedback device*, vol. 4, 2002.

[11] D. S. Walker, D. J. Thoma, and G. Niemeyer, "Variable impedance magnetorheological clutch actuator and telerobotic implementation," in *Intelligent Robots and Systems, 2009. IROS 2009. IEEE/RSJ International Conference on.* IEEE, 2009, pp. 2885–2891.

[12] T. C. Bulea, R. Kobetic, C. S. To, M. L. Audu, J. R. Schnellenberger, and R. J. Triolo, "A variable impedance knee mechanism for controlled stance flexion during pathological gait," *Mechatronics, IEEE/ASME Transactions on*, vol. 17, no. 5, pp. 822–832, 2012.

[13] T. Saito and H. Ikeda, "Development of normally closed type of magnetorheological clutch and its application to safe torque control system of human-collaborative robot," *Journal of Intelligent Material Systems and Structures*, vol. 18, no. 12, pp. 1181–1185, 2007.

[14] J. Oh, B. Drincic, and D. Bernstein, "Nonlinear feedback models of hysteresis," *Control Systems Magazine, IEEE*, vol. 29, no. 1, pp. 100–119, 2009.

[15] D. Hughes and J. T. Wen, "Preisach modeling of piezoceramic and shape memory alloy hysteresis," *Smart Materials and Structures*, vol. 6, no. 3, p. 287, 1997.

[16] D. Batterbee and N. Sims, "Hardware-in-the-loop simulation of magnetorheological dampers for vehicle suspension systems," *Proceedings of the Institution of Mechanical Engineers, Part I: Journal of Systems and Control Engineering*, vol. 221, no. 2, pp. 265–278, 2007.

[17] A. A. Adly, I. D. Mayergoyz, and A. Bergqvist, "Preisach modeling of magnetostrictive hysteresis," *Journal of Applied Physics*, vol. 69, p. 5777, 1991.

[18] P. Yadmellat and M. R. Kermani, "Output torque modeling of a magneto-rheological based actuator," in *World Congress*, vol. 18, no. 1, 2011, pp. 1052–1057.

[19] A. Visintin, *Differential models of hysteresis*. Springer Verlag, 1994.

[20] M. Krasnosel'skii and A. Pokrovskii, *Systems with hysteresis*. English edition Springer, 1989.

[21] P. Yadmellat and M. R. Kermani, "Adaptive modeling of a fully hysteretic magneto-rheological clutch," in *Robotics and Automation (ICRA), 2012 IEEE International Conference on.* IEEE, 2012, pp. 2698–2703.

[22] D. Jiles and D. Atherton, "Ferromagnetic hysteresis," *Magnetics, IEEE Transactions on*, vol. 19, no. 5, pp. 2183–2185, 1983.

[23] M. L. Hodgdon, "Applications of a theory of ferromagnetic hysteresis," *Magnetics, IEEE Transactions on*, vol. 24, no. 1, pp. 218–221, 1988.

[24] C. Jedryczka, P. Sujka, and W. Szelag, "The influence of magnetic hysteresis on magnetorheological fluid clutch operation," *COMPEL: The International Journal for Computation and Mathematics in Electrical and Electronic Engineering*, vol. 28, no. 3, pp. 711–721, 2009.

[25] J. Deur, Z. Herold, and M. Kostelac, "Modeling of electromagnetic circuit of a magnetorheological fluid clutch," in *Control Applications,(CCA) & Intelligent Control,(ISIC), 2009 IEEE.* IEEE, 2009, pp. 113–118.

[26] J. Rabinow, "The magnetic fluid clutch," *American Institute of Electrical Engineers, Transactions of the*, vol. 67, no. 2, pp. 1308–1315, 1948.

[27] K. D. Weiss, T. G. Duclos, J. D. Carlson, M. J. Chrzan, and A. Margida, *High strength magneto-and electro-rheological fluids*. Society of Automotive Engineers, 1993.

[28] M. R. Jolly, J. W. Bender, and J. D. Carlson, "Properties and applications of commercial magnetorheological fluids," *Journal of Intelligent Material Systems and Structures*, vol. 10, no. 1, pp. 5–13, 1999.

[29] J. Carlson and B. Spencer Jr, "Magneto-rheological fluid dampers for semi-active seismic control," in *Proc. of the 3rd Int. Conf. on Motion and Vibr. Control*, 1996, pp. 35–40.

[30] N. M. Wereley and L. Pang, "Nondimensional analysis of semi-active electrorheological and magnetorheological dampers using approximate parallel plate models," *Smart Materials and Structures*, vol. 7, no. 5, p. 732, 1999.

[31] J. D. Carlson and M. R. Jolly, "Mr fluid, foam and elastomer devices," *Mechatronics*, vol. 10, no. 4, pp. 555–569, 2000.

[32] X. Wang and F. Gordaninejad, "Field-controllable electro-and magneto-rheological fluid dampers in flow mode using herschel-bulkley theory," *Damping and Isolation*, vol. 3989, pp. 232–243, 2000.

[33] N. Wereley, J. Cho, Y. Choi, and S. Choi, "Magnetorheological dampers in shear mode," *Smart Materials and Structures*, vol. 17, no. 1, p. 015022, 2007.

[34] S. Hong, N. Wereley, Y. Choi, and S. Choi, "Analytical and experimental validation of a nondimensional bingham model for mixed-mode magnetorheological dampers," *Journal of Sound and Vibration*, vol. 312, no. 3, pp. 399–417, 2008.

[35] D. Wang and T. Wang, "Principle, design and modeling of an integrated relative displacement self-sensing magnetorheological damper based on electromagnetic induction," *Smart Materials and Structures*, vol. 18, no. 9, p. 095025, 2009.

[36] D. Wang and W. Liao, "Magnetorheological fluid dampers a review of parametric modelling," *Smart Materials and Structures*, vol. 20, no. 2, p. 023001, 2011.

[37] A. S. Shafer and M. R. Kermani, "Design and validation of a magneto-rheological clutch for practical control applications in human-friendly manipulation," in *Robotics and Automation (ICRA), 2011 IEEE International Conference on.* IEEE, 2011, pp. 4266–4271.

[38] R. Phillips, "Engineering applications of fluids with a variable yield stress," Ph.D. dissertation, Univ. of California, Berkeley, 1969.

[39] J. Carlson, "What makes a good MR fluid?" *Journal of intelligent material systems and structures*, vol. 13, no. 7-8, p. 431, 2002.

[40] I. H. Shames and F. A. Cozzarelli, *Elastic and Inelastic Stress Analysis*. Englewood Cliffs, New Jersey: Prentice Hall College Div, 1992.